Stabilization of Automotive Vehicles using Active Steering and Adaptive Brake Control Allocation

Johannes Tjønnås and Tor A. Johansen
Department of Engineering Cybernetics, Norwegian University of Science and Technology, Trondheim, Norway
and SINTEF Applied Cybernetics, Trondheim, Norway.

***Abstract*—In this work a dynamic control allocation approach is presented for an automotive vehicle yaw stabilization scheme. The stabilization strategy consists of a high level module that deals with the vehicle motion control objective (yaw rate reference generation and tracking), a low level module that handles the braking control for each wheel (longitudinal slip control and maximal tire-road friction parameter estimation) and an intermediate level dynamic control allocation module that generates the longitudinal slip reference for the low level brake control module and commands front wheel steering angle corrections. The control allocation design is such that the actual torque about the yaw axis tends to the desired torque calculated form the high level module, with desirable distribution of control forces satisfying actuator constraints and minimal control effort objectives.**

Conditions for uniform asymptotic stability are given for the case when the control allocation includes adaptation of the tire-road maximal friction coefficients, and the scheme has been implemented in a realistic non linear multi body vehicle simulation environment. The simulation cases show that the yaw control allocation strategy stabilizes the vehicle in extreme maneuvers where the non linear vehicle yaw dynamics otherwise (without active braking or active steering) becomes unstable in the sense of over- or under steering.

The control allocation implementation is efficient and suitable for low cost automotive electronic control units.

I. Introduction

Some of the major advances in automotive technology in the past decade have been in the area of safety, and most modern passenger vehicles are now equipped with active safety systems. Important components in these systems are Anti-lock Braking Systems (ABS), Traction Control/Anti spin Systems (TCS) and yaw stabilizing systems like the Electronic Stability Program (ESP). ABS and TCS are systems designed to maximize the contact-forces between the tires and the road during braking and acceleration, while ESP is introduced in order to control the yaw motion and prevent over- and/or under steering. There are several ways of controlling the yaw dynamics of a vehicle, for example through an active suspension system [37], or by the torque-biasing system on a four-wheel drive vehicle, where an electronic-controlled limited slip differential (ELSD) [21] is used to transfer the motor torque form the front to the rear axle and between the left and right wheels. But most vehicle stability systems are controlled by active steering, see [1], [2], [3], [20], [5], [8] and references therein, active braking [36], [4] or by a combination of active steering and braking [41], [38], [11] and [9].

The solution to the yaw motion control problem are in [21] and [38] presented in the structure of a control allocation architecture, where a high level controller calculates a desired yaw moment. This yaw rate is then passed to an allocation/distribution module and mapped to desired references for the low level actuator controllers. The advantage of this structure is the modularity of separating the high and low level controls through the introduction of the allocation/distribution algorithm. It is in [28] shown that the knowledge of the friction coefficient offers significant improvement of the vehicle response during yaw rate control. By utilizing vehicle motion information, typical friction coefficient estimation approaches consider either longitudinal or lateral motion measurements, see [24] and references therein. Moreover, depending on sensors, the algorithms in [24] provide estimates of the tire-road friction parameters individually for each wheel, which is useful information for the yaw stabilizing schemes when the road conditions are unknown and non uniform.

In [35] an explicit piecewise linear approximate solution is created by using multi parametric programming and solving the optimization problem off-line, while in [32] a yaw stabilization scheme for an automotive vehicle using brakes, based on the dynamic optimizing control allocation approach from [17] and [34] was presented by the authors. This strategy offers the benefits of a modular approach combining convergence and stability properties for yaw rate tracking (high level control), optimality of the allocation problem and adaptation of the averaged maximal tire-road friction parameter.

In this work we consider the control strategy from [32] and rely on the dynamic control allocation law from [33], which extend the results from [34] by considering actuator dynamics in the control architecture. Furthermore the yaw stabilizing algorithm presented here includes active front wheel steering in combination with low level control of the longitudinal wheel slip and an adaptive law that estimates the maximal tire-road friction parameter for each wheel. In addition to the measurements (yaw rate, steering wheel angle, absolute velocity of the vehicle and wheel side slip) that was necessary in the algorithm from [32], the algorithm presented in this work require measurements (estimates) of the vehicle velocity and angular velocity from each wheel.

In [12] and [22] a quasi-static control allocation problem is solved by a real-time optimizing program, and in [9] the braking and steering actuator commands are generated based on a model predictive control (MPC) formulation which also rely on solving a real-time on line optimization problem numerically. Our approach solve the control allocation problem dynamically (by not necessarily finding the optimal solution at

each sampling instant), such that a real-time implementation can be realized without the use of numeric optimization software. In general, this is an advantage since implementations on vehicles with low-cost hardware may be considered.

The main focus of this report is to show how the adaptive control allocation algorithm from [33] may be applied to optimize the use of redundant actuators in the yaw stabilization problem, formulated in a modular control structure. No direct performance/effectiveness evaluation with respect to other methods is considered in this presentation but from a technical point of view, the main benefits of this approach are: the low memory requirement (no multi parametric program needs to be solved off-line), the low computational complexity (relatively simple dynamic solution without relying on numeric optimization software) and the stability conservation (proved by Lyapunov functions and cascade theory) due to the asymptotic optimality approach. By including adaptive laws for estimating the maximal tire-road friction parameter for each wheel, the yaw stabilizing scheme takes changing road conditions into account, and ultimately the control allocation algorithm will perform better.

The control allocation formulation is flexible and accommodates actuator constraints that can be used also to optimize fault tolerant control performance in response to actuator failure.

The paper is composed as follows: In Section II the control structure is presented. The high level model and controller are derived in section III, while the low level model and controller, along with the qualitative behavior of the tire-road friction model and main design assumptions are given in section IV. The dynamic control allocation strategy is presented in Section V and in Section VI the simulation scenarios are presented and discussed.

II. Control structure

In this section we present the control scheme and its intrinsic modular structure as a solution of the yaw stabilization problem. The main result demonstrates how the computationally efficient dynamic control allocation algorithm, from [33], may be applied as a part of this solution.

The variables and parameters used in this report are explained in Table I and Figures 1 and 2.

The control inputs are in addition to controlling the brake pressure for each wheel, [32], an allied correction of the steering angles of the front wheels ($\Delta\delta_1 := \Delta\delta_2 := \Delta\delta_u$). This means that in total five actuators are available for the control allocation algorithm to manipulate. No steering on the rear wheels is assumed $(\delta_3 := \delta_4 := 0)$.

.

The control allocation approach structurally consists of the following modules (also shown in Figure 3):

1) **The high level yaw rate motion control algorithm.** Based on the vehicle motion model and the driver input $\delta := (\delta_1, \delta_2, 0, 0)^{\mathrm{T}}$, a yaw rate reference r_{ref} is defined and the high level dynamics of the yaw rate error $\tilde{r} := r - r_{ref}$ is described. By treating the virtual control torque M as an available input to the yaw rate system, a virtual control law M_c is designed such that the origin of the error system is Uniformly Globally Asymptotically Stable (UGAS) when $M = M_c$. The reference generator and high level controller rely on (as explained in the next section): the driver input measurement δ, the chassis accelerations a_x and a_y, the wheel side slip angle $\alpha := (\alpha_1, \alpha_2, \alpha_3, \alpha_4)^{\mathrm{T}}$, the vehicle velocity v and the vehicle yaw rate r.
2) **The low level braking control algorithm.** From the dynamics describing the longitudinal wheel slip $\lambda_x := (\lambda_{x1}, \lambda_{x2}, \lambda_{x3}, \lambda_{x4})^{\mathrm{T}}$, a control law for the clamping torque $T_b := (T_{b1}, T_{b2}, T_{b3}, T_{b4})^{\mathrm{T}}$ is de-

i	Subscript for each wheel $i \in [1, 2, 3, 4]$
g	The gravitational constant
High level model	
ν	Absolute speed at the vehicle CG
β	Vehicle side slip angle
ψ	Yaw angle
r	Yaw rate ($\dot{\psi}$)
r_{ref}	Desired Yaw rate
f_x	Force at vehicle CG in longitudinal direction
f_y	Force at vehicle CG in lateral direction
M	Torque about the yaw axis
M_c	Desired torque about the yaw axis
Low level model	
ν_i	Absolute speed at the wheel CG
ν_{xi}	Wheel velocity in the vertical wheel plane
ν_{yi}	Wheel velocity perpendicular to the vertical wheel plane
F_{xi}	Friction force on wheel in longitudinal wheel direction
F_{yi}	Friction force on wheel in lateral wheel direction
F_{zi}	Vertical force on ground from each wheel
δ_i	Steering angle ($\delta_3 := \delta_4 := 0$)
$\Delta\delta_i$	Steering angle correction ($\Delta\delta_3 := \Delta\delta_4 := 0$)
α_i	Wheel side slip angle
λ_{xi}	Wheel slip in longitudinal wheel direction
λ_{xid}	Desired longitudinal wheel slip
ω_i	Angular velocity of wheel i
T_{bi}	Braking torque on each wheel i
Vehicle parameters	
m	Vehicle mass
m_{wi}	Vehicle mass distributed on each wheel i
J_z	Vehicle moment of inertia about the yaw axis
J_ω	Wheel moment of inertial
R	Radius of the wheels
ρ_i	Geometry parameter (see Figure 1)
h_i	Geometry parameter (wheel distance from the CG)
l_i	Geometry parameter (axle distance from CG, $l_1 = l_2$, $l_3 = l_4$)
l	Geometry parameter (rear to front axle distance)
h_c	Geometry parameter (CG height from ground)
a_x	The vehicle chassis backward acceleration
a_y	The vehicle chassis sideways acceleration (opposite from F_{yi})
Environmental parameters	
μ_{Hi}	Maximum tire-road friction coefficient
μ_{yi}	Lateral tire-road friction coefficient
μ_{xi}	Longitudinal tire-road friction coefficient
Some abbreviations	
PE	Persistently excited
US	Uniformly stable
UAS/UES	Uniformly asymptotically/exponentially stable
UGAS/UGES	Uniformly globally asymptotically/exponentially stable
PID	Proportional–integral–derivative controller
MPC	Model predictive control
ABS	Anti-lock braking system
TCS	Traction control system
ESP	Electronic stability program
ELSD	Electronic controlled-limited slip differential

TABLE I
NOMENCLATURE AND MODEL VARIABLES

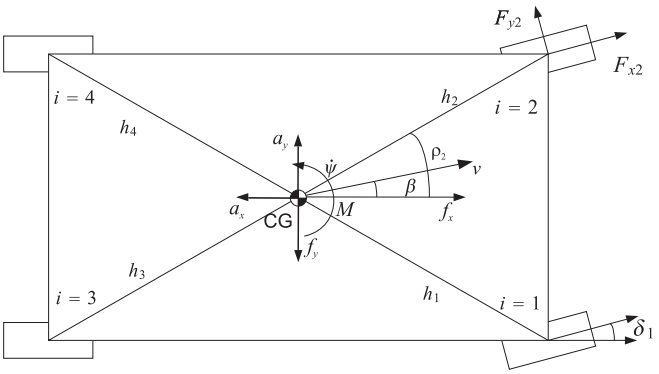

Fig. 1. Vehicle schematic

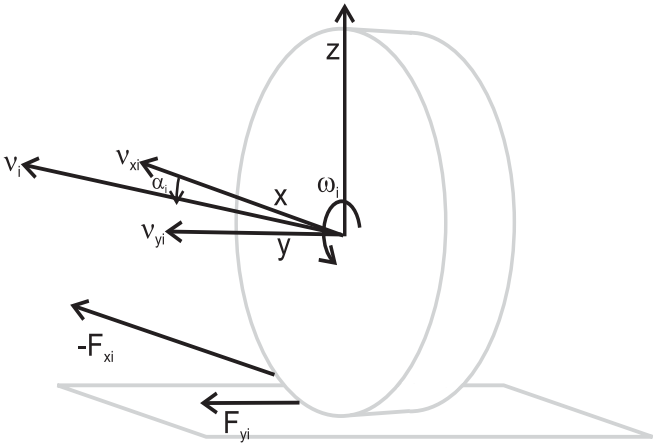

Fig. 2. Quarter car model

fined such that for any smooth reference $\lambda_{xd} := (\lambda_{x1d}, \lambda_{x2d}, \lambda_{x3d}, \lambda_{x4d})^{\mathrm{T}}$, then λ_x will track λ_{xd} asymptotically. The steering dynamics are assumed to be negligible and therefore no low level steering control law is considered. In order to cope with the possibly unknown maximal tire-road friction parameter vector $\mu_H := (\mu_{H1}, \mu_{H2}, \mu_{H3}, \mu_{H4})^{\mathrm{T}}$, appearing in the actuator models, an adaptive law for on line estimation of μ_H is defined. The low level controller that we will utilize is derived in Section IV, and the measurements needed in the algorithm are: the wheel longitudinal slip λ_x, the wheel side slip angle α, the wheel velocity v_i, and the chassis accelerations a_x and a_y.

3) **The dynamic control allocation algorithm (connecting the high and low level controls).** The main objective of the control allocation algorithm is to distribute the desired steering angle correction $\Delta\delta := (\Delta\delta_u, \Delta\delta_u, 0, 0)^{\mathrm{T}}$ and the desired longitudinal wheel slip reference (λ_{xd}) to the low level control, based on the desired virtual control (M_c). The static torque mapping $M = \Phi_M(\delta, \lambda_x, \alpha, \mu_H)$ (see equation (6) for definition) represents the connection between the output of low level system and the input to the high level system. The control allocation problem can be formulated as the static minimization problem

$$\min_{u_d} J(t, u_d) \quad s.t. \;\; M_c - \bar{M}(t, u_d, \hat{\mu}_H) = 0 \;, \qquad (1)$$

where $u_d := (\lambda_{xd}, \Delta\delta_u)$, $\bar{M}(t, u_d, \hat{\mu}_H) := M(\delta(t) + \Delta\delta, \lambda_{xd}, \alpha(t), \hat{\mu}_H)$ and $\hat{\mu}_H$ is an estimate of μ_H. The cost function J is defined such that minimum braking effort and actuator constraints, are incorporated. Based on this formulation, the Lagrangian function

$$L := J(t, u_d) + (M_c - \bar{M}(t, u_d, \hat{\mu}_H))\pi, \qquad (2)$$

is introduced and update-laws for, the steering actuator $\Delta\delta_u$, the longitudinal wheel slip reference λ_{xd} and the Lagrangian parameter π are defined according to the dynamic control allocation algorithm in [33]. The control allocation algorithm depend on the same measurements that are necessary for the high and the low level controllers.

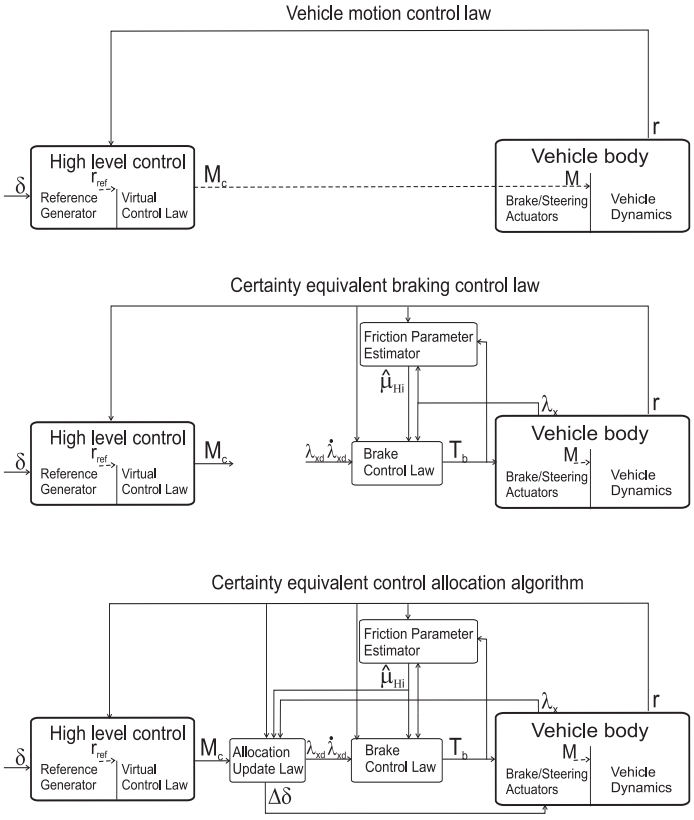

Fig. 3. Adaptive control allocation design philosophy

The benefits of this modular control structure are independence in design, tuning and support of fault tolerant control (e.g. if one actuator fails, the allocation module handle the re-configuration and changed constraints by modifying cost function parameters, without a direct effect on the high level implementation).

Except from the procedure of estimating the tire-road friction parameter, no observer dynamics are included in the analysis or synthesis presented in this paper. This means that all states and variables used in the algorithm are viewed as sampled sensor measurements. However, due to cost and

reliability issues, vehicle velocity and side slip angle are rarely measured directly and observers based on yaw rate, wheel speed, acceleration and steering angle measurements are needed. Simulations of the controlled system using the non linear observers presented in [13] and [14] have been carried out and the results are promising, but left for further work and analysis.

III. High level vehicle model and control design

The dynamic control allocation approach involves modeling of the vehicle over three stages. The high level vehicle motion dynamics, the tire force model and the low level longitudinal wheel slip dynamics.

The high level vehicle motion dynamics

$$\begin{pmatrix} \dot{\nu} \\ \dot{\beta} \\ \dot{r} \end{pmatrix} = -\begin{pmatrix} 0 \\ r \\ 0 \end{pmatrix} + \begin{pmatrix} \frac{1}{m}\cos(\beta) & \frac{1}{m}\sin(\beta) & 0 \\ -\frac{1}{m\nu}\sin(\beta) & \frac{1}{m\nu}\cos(\beta) & 0 \\ 0 & 0 & \frac{1}{J_z} \end{pmatrix} \begin{pmatrix} f_x \\ f_y \\ M \end{pmatrix}, \tag{3}$$

are based on an horizontal plane two-track model that can be found in [19], and serves as the basis for the high level controller design. The generalized forces represented by f_x, f_y and M are defined by the following static mappings also found in [19]:

$$\begin{pmatrix} f_x \\ f_y \end{pmatrix} := \sum_{i=1}^{4} \begin{pmatrix} \cos(\delta_i) & -\sin(\delta_i) \\ \sin(\delta_i) & \cos(\delta_i) \end{pmatrix} \begin{pmatrix} F_{xi} \\ F_{yi} \end{pmatrix} \tag{4}$$

$$M := \Phi_M(\delta, \lambda_x, \alpha, \mu_H) \tag{5}$$

$$\Phi_M := \sum_{i=1}^{4} \begin{pmatrix} -\sin(\rho_i) \\ \cos(\rho_i) \end{pmatrix}^{\mathrm{T}} h_i \begin{pmatrix} \cos(\delta_i) & -\sin(\delta_i) \\ \sin(\delta_i) & \cos(\delta_i) \end{pmatrix} \begin{pmatrix} F_{xi} \\ F_{yi} \end{pmatrix}. \tag{6}$$

A. Vehicle yaw stabilization

The control objective is to prevent the vehicle from over- and/or under steering, i.e. the yaw rate r, of the vehicle should be close to some desired yaw rate r_{ref}, defined by the commanded steering angle. In order to generate this reference the steady-state of the side slip dynamics is considered. Thus from the model (3),

$$\dot{\beta} = -r + \frac{-\sin\beta f_x + \cos\beta f_y}{m\nu},$$

the desired reference is generated by letting $\dot{\beta} = \beta = 0$ and $\lambda_x = 0$, such that:

$$r_{ref} := \frac{f_y(a_x, a_y, \alpha, \lambda_x = 0, \delta, \mu_{nH})}{m\nu}, \tag{7}$$

where μ_{nH} is a tuning parameter for the maximal tire-road friction parameter. Hence, if the vehicle follows this yaw rate reference, the driver will experience a yaw motion related to a virtual desired surface described by μ_{nH}. Another approach could be to use the maximal tire-road friction coefficient estimate $\hat{\mu}_H$ (or a weighted average of $\hat{\mu}_{Hi}$ from each wheel) to generate $\mu_{nH} := \mu_{nH0} + \hat{\mu}_H$, where $\mu_{nH0} > 0$ in (7). If $\hat{\mu}_H$ is in close proximity of μ_H, then the approach will generate feasible yaw rate references. On the other hand if big transients occur, unstable yaw motion may be introduced by this reference generation. By fixing μ_{nH}, a conservative approach is taken and non "optimal" yaw rate references may be generated for high friction surfaces, but no undesired transients are introduced by the reference generator.

Remark 1 *Note that at $\nu = 0$ the yaw rate reference generation has a singularity, which means that (7) is not suitable for low speeds. This problem is avoided by introducing a threshold $\nu_T > 0$ such that the algorithm is only active at $\nu > \nu_T$, which is a common limitation of wheel slip control, see e.g. [18].*

Moreover the yaw rate reference model is generated by setting the vehicle side slip angle to zero, e.g. it is assumed that the driver does not want to follow a reference based on, or compensating for, side slip motion. Many yaw rate reference models are proposed in literature, most rely on the lateral velocity and steering angle input parameters, see for example the second order model in [38], and the model in [23] where a reference for desired vehicle side slip is presented. Such methods are based on stability factors or under-steer gradients. The main focus of this paper is on the control allocation and a simplified yaw rate reference generator with a tuning parameter μ_{nH}, related to the road surface conditions, is considered. But based on the modular control structure, any yaw rate reference generator may in general be considered.

For safe driving such as rollover prevention and vehicle controllability conservation ([19]), the side-slip angle should be limited by

$$|\beta| \leq 10^\circ - 7^\circ \frac{\nu^2}{(40[m/s])^2}. \tag{8}$$

Although this bound is not explicitly enforced in this scheme, simulations show that due to the yaw rate reference tracking (founded on zero side slip), the side slip angle satisfies (8).

The high level control design is based on the reduced model from (3):

$$\dot{r} = \frac{M}{J_z}. \tag{9}$$

Let $\tilde{r} := r - r_{ref}$ denote the yaw rate error such that a virtual tracking PI controller can be described by

$$M_c(t, \tilde{r}, e_r) := -K_P\tilde{r} - K_I e_r + J_z\dot{r}_{ref} \tag{10}$$

where

$$\dot{e}_r = \tilde{r} \tag{11}$$

$$\dot{\tilde{r}} = \frac{M}{J_z} - \dot{r}_{ref} = -\frac{K_P}{J_z}\tilde{r} - \frac{K_I}{J_z}e_r + \frac{M - M_c}{J_z}. \tag{12}$$

With $M = M_c$ the linear tracking error dynamics become:

$$\dot{e}_r = \tilde{r} \tag{13}$$

$$\dot{\tilde{r}} = -\frac{K_P}{J_z}\tilde{r} - \frac{K_I}{J_z}e_r, \tag{14}$$

and clearly the equilibrium $(\tilde{r}, e_r) = 0$ of (13)-(14) is Uniformly Globally Exponentially Stable (UGES) for $K_P, K_I > 0$.

IV. Low level model and controller

In the literature, different wheel slip definitions are used. For example in [6] the longitudinal wheel slip is defined in the wheel absolute velocity direction, while in [25] the longitudinal wheel slip is defined in the wheel vertical plane. The definitions also vary related to the drive or braking modes. We use the following longitudinal and lateral wheel slip definitions:

$$\lambda_{xi} := \frac{\nu_{xi} - \omega_i R}{\nu_i}, \ \lambda_{yi} := \sin(\alpha_i), \tag{15}$$

$$\nu_i = \sqrt{\nu_{xi}^2 + \nu_{yi}^2}, \tag{16}$$

where the longitudinal wheel slip is given in the wheel vertical plane. The parameter α_i is throughout this work treated as a measurement or estimate. The friction model is parameterized by α_i rather then λ_{yi}.

From the wheel slip definitions and the horizontal quarter car model,

$$J_\omega \dot{\omega}_i = -RF_{xi} - T_{bi} sign(\omega_i),$$

the following low level longitudinal wheel slip dynamics is derived, (see [31]), assuming $J_\omega \ll R^2 m_{wi}$ (typical for standard cars)

$$\dot{\lambda}_{xi} = \frac{R}{\nu_i J_\omega} \left(sign(\omega_i) T_{bi} - \phi_i(F_{zi}, \lambda_{xi}, \alpha_i, \mu_{Hi}) \right), \tag{17}$$

where

$$\phi_i(F_{zi}, \lambda_{xi}, \alpha_i, \mu_{Hi}) := RF_{zi} \mu_{xi}(\lambda_{xi}, \alpha_i, \mu_{Hi}),$$

Note that also the low level wheel slip model has a singularity at $\nu_i = 0$, but since in principle a yaw stabilizing algorithm is not needed in a region around this singularity, a threshold will be introduced in order to switch off the algorithm (see remark 1). The model of the forces generated at the contact point between the tire and the road, represented by F_{xi} and F_{yi} i.e. the friction coefficients μ_{xi} and μ_{yi}, are considered in the following.

A. Tire-road friction model

The longitudinal and lateral friction forces acting on the tires are described by the product between the normal forces and the friction coefficients:

$$F_{xi}(F_{zi}, \lambda_{xi}, \alpha_i, \mu_{Hi}) := -F_{zi} \mu_{xi}(\lambda_{xi}, \alpha_i, \mu_{Hi}) \tag{18}$$

$$F_{yi}(F_{zi}, \lambda_{xi}, \alpha_i, \mu_{Hi}) := -F_{zi} \mu_{yi}(\lambda_{xi}, \alpha_i, \mu_{Hi}). \tag{19}$$

The normal force on each tire is calculated through measuring the chassis accelerations a_x and a_y, by assuming that the coupling between roll and pitch and the suspension dynamics can be neglected:

$$F_{zi} := m \left(\frac{l_i g - h_c a_x}{l} \right) \left(\frac{1}{2} - \frac{h_c a_y}{\sqrt{h_i^2 - l_i^2}} \right), \tag{20}$$

where equation (20) can be found in for example [19]. In Figure 4 and 5 the friction coefficients that are used in the presented control allocation algorithm are illustrated with dependence on the longitudinal wheel slip, the maximal tire-road friction parameter and the wheel side slip angle. The control allocation approach we present, do not rely strongly on the detailed structure of the tire-road friction model, but certain qualitative properties are required, and the model should be parameterized according to the tire quality in order to give good friction force predictions.

(i) $\frac{\partial \mu_{xi}}{\partial \lambda_{xi}} > 0$, for small longitudinal slips.

(ii) $\frac{\partial \mu_{xi}}{\partial \mu_{Hi}} > 0$ and $\frac{\partial \mu_{yi}}{\partial \mu_{Hi}} > 0$ for sufficiently large longitudinal slip.

(iii) The first order partial derivatives of the friction coefficients (μ_{xi} and μ_{yi}) with respect to the maximal tire-road friction, dominate the higher order partial derivatives.

The first assumption (i) states that in a certain region defined by the longitudinal wheel slip (λ_{xi}), the wheel side slip (α_i) and the maximal tire-road friction parameter (μ_{Hi}), the longitudinal friction coefficient (μ_{xi}) is strictly increasing with respect to λ_{xi}, for fixed α_i and μ_{Hi}. This assumption is needed in the control allocation algorithm in order to guarantee convex solutions and in the definition of the control variable bounds. The second assumption (ii) requires that in a region defined by λ_{xi}, α_i and μ_{Hi}, the friction coefficients both in longitudinal and lateral direction are strictly increasing with respect to the maximal tire-road fiction parameter. The last assumption (iii) is a technical assumption, used in the analysis to prove parameter convergence ($\hat{\mu}_{Hi} \to \mu_{Hi}$) through Persistence of Excitation (PE) arguments (defined in section IV.C). For additional technical assumptions that guarantee parameter convergence see [31]. These assumptions are typically satisfied (for a given range of longitudinal wheel slip) in general friction models such as Pacejka's magic formula and Burckharts approach [6].

In Figure 4 and 5.

B. Wheel slip dynamics

In this section an approximation of the wheel slip dynamics is presented. The analysis and control design are limited to the cases where the vehicle always has forward speed, the wheels are never rotating in reverse and the wheels are always fixed on the ground. The following approximation, simplify the control design, the allocation algorithm and the analysis.

Approximation 1 *From the above assumption (iii) and the Taylor approximation, it can be shown that the model*

$$\bar{\phi}_i(F_{zi}, \lambda_{xi}, \alpha_i, \hat{\mu}_{Hi}) := \left. \frac{\partial \phi_i(F_{zi}, \lambda_{xi}, \alpha_i, s_i)}{\partial s_i} \right|_{s_i = \hat{\mu}_{Hi}},$$

enables an approximation of the force difference between the real and the estimated tire-road friction forces. I.e.

$$\begin{aligned} \bar{\phi}_i(F_{zi}, \lambda_{xi}, \alpha_i, \hat{\mu}_{Hi}) \tilde{\mu}_{Hi} \approx \phi_i(F_{zi}, \lambda_{xi}, \alpha_i, \mu_{Hi}) \\ - \phi_i(F_{zi}, \lambda_{xi}, \alpha_i, \hat{\mu}_{Hi}), \end{aligned}$$

where $\tilde{\mu}_{Hi} := \mu_{Hi} - \hat{\mu}_{Hi}$.

From the Approximation 1, the longitudinal wheel slip dynamic may be simplified such that the maximal tire-road

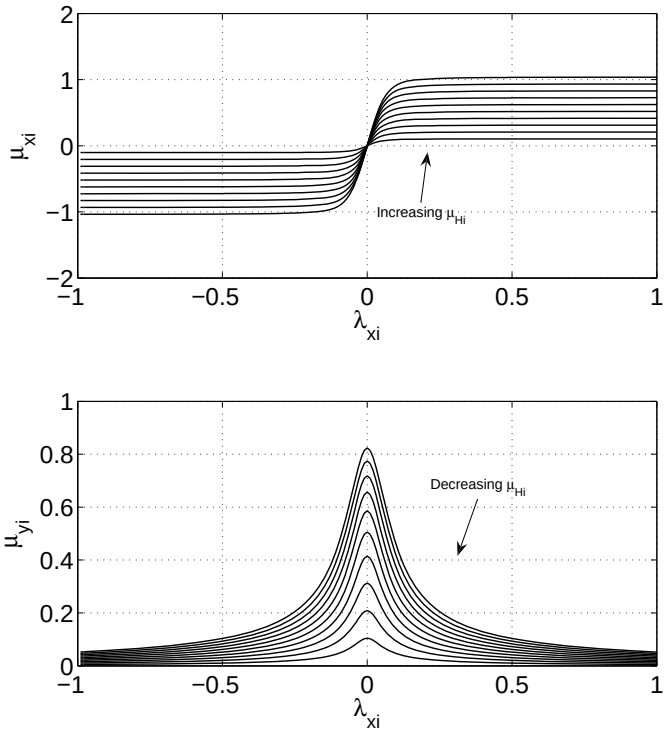

Fig. 4. The mapping from longitudinal wheel slip λ_{xi} to forces in longitudinal μ_{xi} and lateral μ_{yi} direction affected by changes in the maximal tire road friction coefficient μ_{Hi}. $\alpha_i = 3[\text{deg}]$

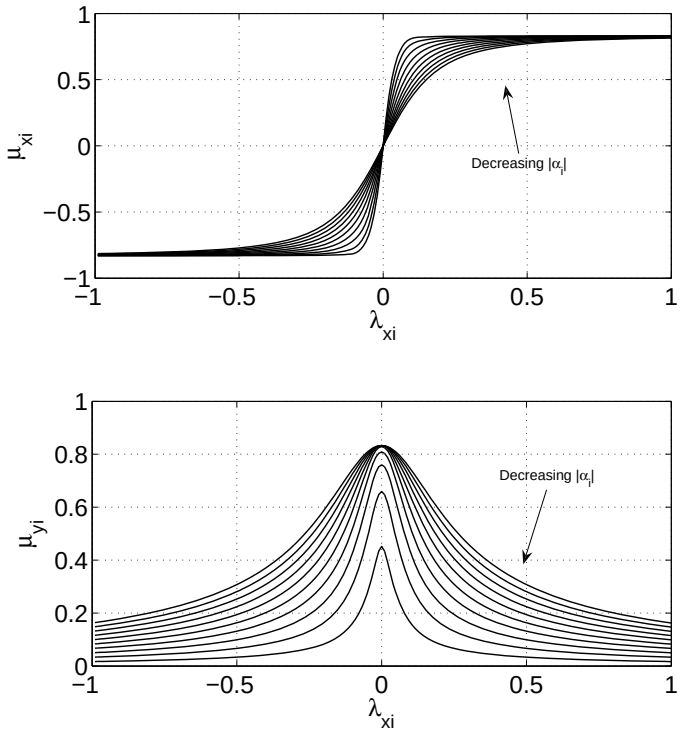

Fig. 5. The mapping from longitudinal wheel slip λ_{xi} to forces in longitudinal μ_{xi} and lateral μ_{yi} direction affected by the changes the wheel side slip α_i. $\mu_{Hi} = 0.8$

friction parameter appear affinely in the model.

$$\dot{\lambda}_{xi} = -\frac{R}{\nu_i J}\phi_i(F_{zi}, \lambda_{xi}, \alpha_i, \hat{\mu}_{Hi}) + \frac{R}{\nu_i J}\left(-\bar{\phi}_i(F_{zi}, \lambda_{xi}, \alpha_i, \hat{\mu}_{Hi})\tilde{\mu}_{Hi} + T_{bi}\right). \quad (21)$$

C. Low level wheel slip control

In the control synthesis that we present, the low level system is described by the longitudinal wheel slip dynamic such that slip control laws developed for anti-lock brake systems (ABS) may be used. When the ABS is active its main purpose is to maximize the friction force between the road and the tires. For given μ_{Hi} and α_i these maximal forces are uniquely defined by the fixed desired longitudinal wheel slip. In a yaw stabilizing scheme the desired longitudinal wheel slip is not fixed and a reference tracking controller is needed.

Different control allocation strategies/approaches may be considered, for example one may define the longitudinal wheel forces F_{xi} as the allocation variables, in stead of longitudinal wheel slips λ_{xi} (F_{yi} will then be modeled as a function of F_{xi}). This approach may simplify the control allocation design when no low level dynamics are considered (generating reference forces to the independent braking and steering modules). But when the slip dynamics becomes significant the control allocation design becomes more involved as the feasible force constraints and references are time-varying (dependent on the wheel side slip angle) and as the wheel slip dynamics need to be handled directly in the control allocation algorithm, and the calculation of feasible force constraints.

The low level control objective is based on the longitudinal wheel slip error dynamics derived from equation (21):

$$\dot{\tilde{\lambda}}_{xi} = -\frac{R}{\nu_i J_z}\phi_i(F_{zi}, \lambda_{xi}, \alpha_i, \hat{\mu}_{Hi}) - \dot{\lambda}_{xid} + \frac{R}{\nu_i J_z}\left(-\bar{\phi}_i(F_{zi}, \lambda_{xi}, \alpha_i, \hat{\mu}_{Hi})\tilde{\mu}_{Hi} + T_{bi}\right), \quad (22)$$

where $\tilde{\lambda}_{xi} := \lambda_{xi} - \lambda_{xid}$. Many different wheel slip control strategies can be found in the literature; see for example the mixed slip-deceleration approach from [26], Lyapunov based solutions [10], [40] and [18], sliding-mode based controllers [7], [39] and [27] and PID approaches [30], [16] and [29]. Here we consider a standard Lyapunov approach with adaptation and feed-forward which allows a straight forward use of the dynamic control allocation result from [33].

Based on the Lyapunov function candidate

$$V_{\lambda i}(\tilde{\lambda}_{xi}, \bar{\lambda}_{xi}, \tilde{\mu}_{Hi}) := \frac{1}{2}\left(\tilde{\lambda}_{xi}^2 + \gamma_{\bar{\lambda}i}\bar{\lambda}_{xi}^2 + \gamma_{\mu i}\tilde{\mu}_{Hi}^2\right), \quad (23)$$

when μ_{Hi} is not known, the following adaptive laws (maximal tire road friction parameter estimator) and certainty equivalent wheel slip control laws are suggested:

$$\dot{\hat{\mu}}_{Hi} = -\gamma_{\mu i}^{-1}\frac{R}{\nu_i J_z}\bar{\phi}_i(F_{zi}, \lambda_{xi}, \alpha_i, \hat{\mu}_{Hi})\left(\tilde{\lambda}_{xi} + \gamma_{\bar{\lambda}i}\bar{\lambda}_{xi}\right) \quad (24)$$

$$T_{bi} := \phi_i(F_{zi}, \lambda_{xi}, \alpha_i, \hat{\mu}_{Hi}) + \frac{\nu_i J_z}{R}\dot{\lambda}_{xid} - \frac{\nu_i J_z}{R}\Gamma_P\tilde{\lambda}_{xi} \quad (25)$$

where $\bar{\lambda}_{xi} := \lambda_{xi} - \hat{\lambda}_{xi}$ and

$$\dot{\hat{\lambda}}_{xi} = A\left(\lambda_{xi} - \hat{\lambda}_{xi}\right) + \frac{R}{\nu_i J_z}\left(T_{bi} - \phi_i(F_{zi}, \lambda_{xi}, \alpha_i, \hat{\mu}_{Hi})\right) \tag{26}$$

where $-A$ is a Hurwitz matrix defining the convergence rate of the error estimate, and Γ_P is a positive definite matrix.

The estimation of the maximal tire-road friction parameter (μ_{Hi}) for each wheel enables a more precise friction coefficient estimates (μ_{xi} and μ_{yi}) which is important in order to allocate the high level controls in a optimal way. Other tire-road friction estimation strategies may be considered e.g. [24]. The adaptive scheme presented in the paper has the standard gradient structure $\dot{\hat{\theta}} = \Gamma\Phi\epsilon$ (see for example [15]), where $\hat{\theta}$ is the parameter estimate, Γ is the tuning gain, Φ is the regression vector and ϵ represents the error between the a measured and an estimated state. This structure enables a simple Lyapunov analysis.

Under some technical assumptions, the equilibrium $(\tilde{\lambda}_{xi}, \bar{\lambda}_{xi}, \tilde{\mu}_{Hi}) = 0$ for the system (22), (24) and (26) and the controller (25) is US. If in addition $\bar{\Phi}_i(t) := \frac{R}{\nu_i(t)J_z}\bar{\phi}_i(\lambda_{xi}(t), \alpha_i(t), \hat{\mu}_{Hi}(t))$ is PE, i.e. let $\bar{\Phi}_i(t)$ be a time-varying function then there exist constants T and $\gamma > 0$, such that

$$\int_t^{t+T} \bar{\Phi}_i(\tau)^{\mathrm{T}}\bar{\Phi}_i(\tau)d\tau \geq \gamma I \ , \quad \forall t > t_0,$$

then the equilibrium $(\tilde{\lambda}_{xi}, \bar{\lambda}_{xi}, \tilde{\mu}_{Hi}) = 0$ is UAS with respect to the system (22), (24) and (26) and the controller (25). See [31] for detailed proofs.

Notice that if the wheels are not longitudinally slipping, $\bar{\Phi}_i(t)$ will not be persistently excited, such that convergence of the maximal tire-road friction parameters can not be guaranteed.

V. The control allocation algorithm

We have chosen a fairly straight forward Lyapunov based design both for the high level yaw stabilizing controller and the low level longitudinal wheel slip controller. Other controllers may be applied as long as uniform asymptotic stability is achieved. The performance of the high and low level controllers are crucial in order to solve the yaw stabilizing problem, but the main contribution of this work is to show how the dynamic control allocation algorithm may be used for coordinating the actuators without the use of additional optimizing software. In the following we present the control allocation algorithm based on the strategy from section II, by considering the approach from [33] and [31].

The basis of the control allocation algorithm lies in finding an update law for the longitudinal wheel slip (λ_{xid}) and the steering angle correction ($\Delta\delta_i$) that asymptotically solves the optimization problem (1), where (4)-(6) defines the equality constraint and $J(t, u_d)$ defines the objectives that one wants to minimize. Typically the cost function capture objectives that; minimize energy or power consumption, handle input/actuator constraints and avoid singularities. We consider the instantaneous cost function that is divided into two parts $J(u_d) := J_1(u_d) + J_2(u_d)$, where the function $J_1(u_d)$ represents the actuator penalty and $J_2(u_d)$ is a barrier function representation of the actuator constraints.

$$J_1(u_d) := u_d^{\mathrm{T}} W_u u_d \tag{27}$$

$$\begin{aligned} J_2(u_d) := &-w_\lambda \sum_{i=1}^{4} \ln(\lambda_{xid} - \lambda_{x\min}) - w_\lambda \sum_{i=1}^{4} \ln(-\lambda_{xid} + \lambda_{x\max}) \\ &-w_\delta \sum_{i=1}^{2} \ln(\Delta\delta_i + \Delta\delta_{\min}) - w_\delta \sum_{i=1}^{2} \ln(-\Delta\delta_i + \Delta\delta_{\max}), \end{aligned} \tag{28}$$

where $\lambda_{x\max}$, $\lambda_{x\min}$, $\Delta\delta_{\max}$, and $\Delta\delta_{\min}$ are wheel-slip and steering angle constraints. w_λ and w_δ are positive parameters that defines the barrier function slopes which become significant as the actuators approach their constraints, while W_u is a positive definite weighting matrix that defines how the high level control should be distributed among the brakes and the steering angle correction. Also, $W_u = W_u(t)$ may be time varying, such that the weighting may depend on the driver inputs or driving conditions. For instance, sudden large changes in δ, together with heavy braking may indicate a safety critical situation and W_u should reflect a prioritization of the brakes, contra the steering angle correction. If the situation is less critical, the steering angle correction can be prioritized for increased comfort and a smaller velocity drop (higher joy of ride). In the case of high friction surface and high speed, sharp steering maneuvers may also trigger rollover, such that a reduction in the lateral forces by using the brakes may be preferable. An in-depth study on how W_u reflects safety critical situations is not carried out, such that the simulations are done only for the simple cases where W_u is constant.

Let the high level dynamics be defined by $x := (e_r, \tilde{r})^{\mathrm{T}}$, $g := (0, \frac{1}{J_z})^{\mathrm{T}}$ and $f(t, x) := (\tilde{r}, -K_p\tilde{r} - K_i e_r)^{\mathrm{T}}$. With reference to Chapter 5 in [31], the following certainty equivalent dynamic control allocation algorithm is constructed based on; the Lagrangian function (2), the high level control law (10), the adaptive law (24) and the certainty equivalent low level control law (25):

$$\left(\dot{u}_d^{\mathrm{T}}, \dot{\pi}^{\mathrm{T}}\right)^{\mathrm{T}} = -\gamma(t)\left(\mathbb{H}^{\mathrm{T}} W_\pi \mathbb{H}\right)^{-1}\mathbb{H}\left(\frac{\partial L}{\partial u_d}^{\mathrm{T}}, \frac{\partial L}{\partial \pi}^{\mathrm{T}}\right)^{\mathrm{T}} - \mathbb{H}^{-1} u_{dff}, \tag{29}$$

$$\begin{aligned} \dot{\hat{\mu}}_{Hi} = &-\gamma_{\mu i}^{-1}\bar{\Phi}_i^{\mathrm{T}}(\lambda_x, \alpha, \hat{\mu}_H, \nu)\left(\tilde{\lambda}_{xi} + \gamma_{\bar{\lambda}i}^{-1}\bar{\lambda}_{xi}\right) \\ &+ \gamma_{\mu i}^{-1}\bar{\Phi}_{Mi}^{\mathrm{T}}(\delta, \lambda_x, \alpha, \hat{\mu}_H) g^{\mathrm{T}} \frac{\partial^2 L^{\mathrm{T}}}{\partial x \partial \pi}\frac{\partial L}{\partial \pi}. \end{aligned} \tag{30}$$

The first part of equation (29) represents a part that ensures convergence and stability, while u_{dff}, given by:

$$\begin{aligned} u_{dff} := &\left(\frac{\partial^2 L}{\partial t \partial u_d}^{\mathrm{T}}, \frac{\partial^2 L}{\partial t \partial \pi}^{\mathrm{T}}\right)^{\mathrm{T}} + \left(\frac{\partial^2 L}{\partial x \partial u_d}^{\mathrm{T}}, \frac{\partial^2 L}{\partial x \partial \pi}^{\mathrm{T}}\right)^{\mathrm{T}} f(t, x) \\ &+ \left(\frac{\partial^2 L^{\mathrm{T}}}{\partial x \partial u_d}, \frac{\partial^2 L^{\mathrm{T}}}{\partial x \partial \pi}\right)^{\mathrm{T}} g \frac{1}{J_z}\bar{M}(t, u_d, \hat{\mu}_H) \\ &+ \left(\frac{\partial^2 L^{\mathrm{T}}}{\partial \hat{\mu}_H \partial u_d}, \frac{\partial^2 L^{\mathrm{T}}}{\partial \hat{\mu}_H \partial \pi}\right)^{\mathrm{T}} \Gamma_{\mu}^{-1}\left(\tilde{\lambda}_{xi} + \Gamma_{\bar{\lambda}}^{-1}\bar{\lambda}_{xi}\right)\bar{\Phi}(\lambda_x, \alpha, \hat{\mu}_H) \end{aligned} \tag{31}$$

represents a feed-forward like term introduced to ensure invariance of the time-varying optimal equilibrium set. Furthermore, $\bar{\Phi}_i(\lambda_x, \alpha, \hat{\mu}_H) := \frac{R}{\nu_i J_z}\bar{\phi}_i(F_{zi}, \lambda_{xi}, \alpha_i, \hat{\mu}_{Hi}))$, $\bar{\Phi}(\lambda_x, \alpha, \hat{\mu}_H) := diag(\bar{\Phi}_i(\lambda_x, \alpha, \hat{\mu}_H))$, $\bar{\Phi}_{Mi}(\delta, \lambda_x, \alpha, \hat{\mu}_H) := \frac{\partial \Phi_M(\delta, \lambda_x, \alpha, \hat{\mu}_H)}{\partial \hat{\mu}_{Hi}}$, $\Gamma_\mu^{-1} := diag(\gamma_{\mu i}^{-1})$, $\Gamma_{\bar{\lambda}}^{-1} := diag(\gamma_{\bar{\lambda} i}^{-1})$, $\mathbb{H} := \begin{pmatrix} \frac{\partial^2 L}{\partial u_d^2} & \frac{\partial^2 L}{\partial \pi \partial u_d} \\ \frac{\partial^2 L}{\partial u_d \partial \pi} & 0 \end{pmatrix}$, $W_\pi > 0$, and $\gamma(t) = \gamma^{\mathrm{T}}(t)$ is a positive definite time-varying weighting matrix that ensures numerical feasibility. Together with W_u, the weighting matrix W_π represents the main tuning parameter of the control allocation algorithm. W_π defines the prioritization between the minimization of $\left|\frac{\partial L}{\partial \pi}\right|$ (the control error $\left|M_c - \bar{M}\right|$) compared to $\left|\frac{\partial L}{\partial u_d}\right|$ (the deviation of the control inputs with respect to the optimal solution). In practice, if W_u is diagonal, a high value of the last element in W_u compared to the remaining elements, imply that $\bar{M}$ will converge faster to M_c, but at the cost of non-optimal (with respect to the cost function J) use of actuator control effort.

Consider the optimal equilibrium set of the closed loop (11), (12), (22), (26), (24) and (29). It is defined by the variables x, u_d, $\tilde{\lambda}_x$, π, $\bar{\lambda}_x$, $\tilde{\mu}_H$ that satisfy $x = 0$, $\frac{\partial L}{\partial u_d} = 0$, $\frac{\partial L}{\partial \pi} = 0$, $\tilde{\lambda}_x = 0$, $\bar{\lambda}_x = 0$, $\tilde{\mu}_{Hi} = 0$. From the Lyapunov function candidate

$$V_{u_d \pi \tilde{u} \eta \tilde{\theta}}(t, x(t), u_d, \pi, \tilde{u}, \tilde{\lambda}_{xi}, \bar{\lambda}_{xi}, \tilde{\mu}_H) := V_{\lambda i}(\tilde{\lambda}_{xi}, \bar{\lambda}_{xi}, \tilde{\mu}_{Hi}) + \frac{1}{2}\left(\frac{\partial L^{\mathrm{T}}}{\partial u_d}\frac{\partial L}{\partial u_d} + \frac{\partial L_{\hat{\theta}}^{\mathrm{T}}}{\partial \pi}\frac{\partial L_{\hat{\theta}}}{\partial \pi}\right), \quad (32)$$

it can be shown under additional technical assumptions that the equilibrium set is uniformly asymptotically stable, [33].

Based on this analysis we have a local solution where u converges asymptotically to u_d, u_d converges asymptotically to the optimal solution of problem (1) and $\hat{\mu}_H$ converges asymptotically to μ_H (as long as the wheels are slipping), such that M converges asymptotically to M_c and finally r converges to r_{ref} in a stable sense, which is the main goal of this work.

Since the control allocation algorithm (29) and (30) incorporate feed forward terms, signal noise and model errors may influence on the performance of the algorithm**,** such that the simulator should incorporate realistic actuator and measurement behavior (noise and error sources).

Furthermore this result is also valid for the special cases where the number of actuators available may be reduced to:

- only braking actuators, or
- only steering actuator.

Other special cases can also be formulated and handled by the control allocation algorithm. This gives considerable flexibility to optimize performance in various conditions, including fault tolerant control in case of a single brake actuator or steering actuator failure.

VI. Simulation results

In order to validate the yaw stabilization scheme, a testbench based on DaimlerChrysler's proprietary 6DOF multibody simulation environment, with suspension dynamics, CASCaDE (Computer Aided Simulation of Car, Driver and Environment) for MATLAB, is used. Three simulation scenarios are investigated:

- **Understeering:** The understeered motion is a "stable" but not desired yaw motion of the vehicle. It is defined by the yaw rate being less then the desired yaw rate i.e. $|r| < |r_{ref}|$. Typically such behavior appear on low friction surfaces during relatively fast but limited steering maneuvers. In Figure 6 the initial conditions and behavior of the uncontrolled periodically understeered vehicle is presented undergoing a sinusoidal steering maneuver on a surface with the maximal tire-road friction $\mu_{Hi} = 0.3$ for $i \in \{1, 2, 3, 4\}$.

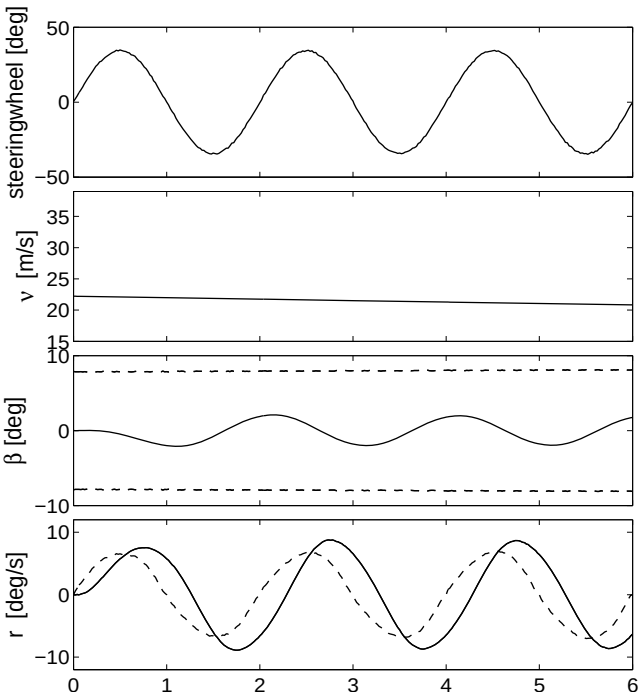

Fig. 6. The steering maneuver and states of an periodically understeered vehicle (no active yaw stabilization). The dashed lines are given by r_{ref} (7) and $\beta_{\max}$(8).

- **Oversteering:** The over steered motion is an "unstable" motion of the vehicle where the yaw rate is greater than the desired yaw rate i.e. $|r| > |r_{ref}|$. In Figure 7 an uncontrolled over steered maneuver is created by a slow increasing left going steering wheel motion. The maximal tire-road friction is $\mu_{Hi} = 0.7$ for $i \in \{1, 2, 3, 4\}$.
- **Fishhook:** The Fishhook maneuver is motivated by a vehicle changing lanes. In this scenario the maximal tire-road friction is initially $\mu_{Hi} = 0.9$ for $i \in \{1, 2, 3, 4\}$ (dry asphalt), but at ca. $1.6s$ the maximal tire-road friction parameter changes to $\mu_{Hi} = 0.3$ for $i \in \{1, 2, 3, 4\}$ (wet/snowy surface). The initial conditions are given in the Figure 8.

Realistic actuator and measurement properties used in the simulations are summarized in Table II, where the noise properties are represented by the precision parameter that defines the bandwidth of white noise with a flat power spectral density. . The vehicle measurements and the yaw stabilization

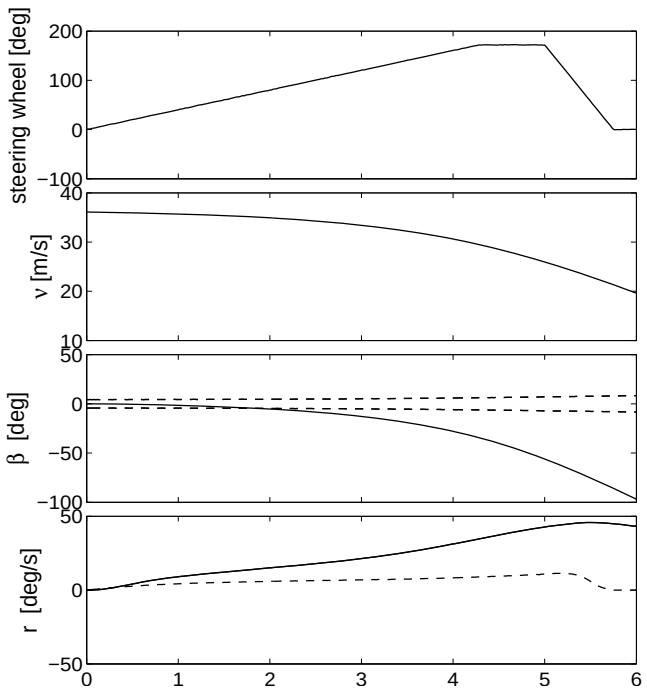

Fig. 7. The steering maneuver and states of an over steered vehicle (no active yaw stabilization). The dashed lines are given by r_{ref} (7) and $\beta_{\max}$(8).

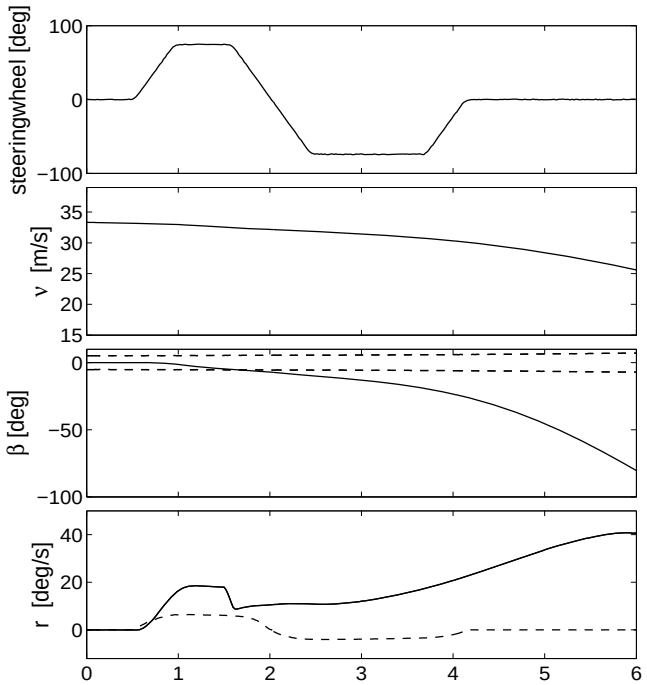

Fig. 8. The fishhook steering maneuver and related vehicle states (no active yaw stabilization). The dashed lines are given by r_{ref} (7) and $\beta_{\max}$(8).

algorithm are operated with a $50Hz$ sampling rate. Moreover the brake pressure commands are delayed with 0.02 seconds in order to simulate the effect of communication and computer delays, and dynamics of the actuators. The algorithm parameters used in the simulations are given by Table III; ε ensures singularity avoidance in (29) where $\mathbb{H}$ is replaced with $\mathbb{H}+\epsilon I$, W_π is a weighting matrix penalizing the error

Actuator constraints (brake pressure)		
Maximum pressure	200 [bar]	
$\max$ pressure-buildup time 0..50 [bar]	0.2 [s]	
buildup time 0..100 [bar]	0.5 [s]	
reduction rate	-1000 [bar/s]	
Measurement	**Resolution**	**Precision**
δ_i	0.1 [deg]	0.5 [deg]
ν	0.0007 [m/s]	0.28 [m/s]
β	0.28 [deg]	0.5 [deg]
$\dot{\psi}$	0.28 [deg/s]	0.5 [deg]
α_i	0.0001 [deg]	0.003[deg]
λ_{xi}	0.0001	0.0005

TABLE II

of $\left|M_c - \bar{M}\right|$ against $\left|\frac{\partial L}{\partial \lambda_{xd}}\right|$, W_u defines the quadratic cost function of problem (1) and w_λ and w_δ defines the steepness of the barrier function (28). The control and adaptive algorithm parameters are tuned based on simulations. The longitudinal wheel slip constraints are chosen with respect to the system requirements (no wheel acceleration/negative longitudinal slip can be commanded). $\Delta\delta_{\max}$ and the fifth element of W_u may be driver style dependent parameters. A high value $\Delta\delta_{\max}$ and a low value of the fifth element of W_u compared with the remaining elements of W_u, indicate that most of the control effort will rely on the steering angle manipulation and result in a yaw stabilizing steer-by-wire algorithm.

The initial estimate of the maximal tire-road friction parameter is $\hat{\mu}_{Hi} = 0.5$ for $i \in \{1, 2, 3, 4\}$ so that the adaptive mechanism of the algorithm is shown both for initial under and over estimation. The nominal maximal tire-road friction coefficient that describes the virtual reference surface (7) is given by $\mu_{nH} = 0.7$. In order to prevent estimator windup, the adaptive algorithm (30) is only active when $\bar{\Phi}_i$ is PE. PE of $\bar{\Phi}_i$ is ensured by only considering adaptation in situations with sufficiently large longitudinal wheel slip, i.e. $\lambda_{xi} > \lambda_{Axi} > 0$ where λ_{Axi} is given in Table III.

Furthermore, in order to prevent the allocation update law (29) from generating infeasible actuator commands, due to the discretization of the system, γ is chosen to be a diagonal matrix where each element represents a positive step length that is made as small as necessary to achieve feasibility.

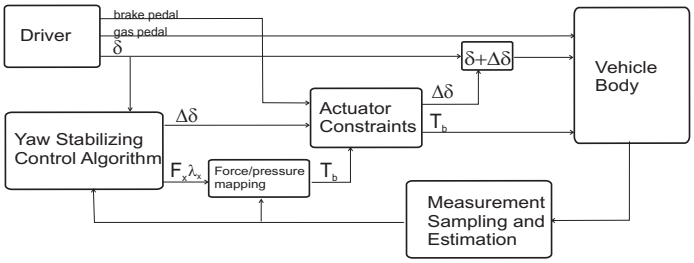

Fig. 9. Block diagram of the simulation setup

The CASCaDE model (see Figure 9) control inputs are defined through the steering angle (manipulated with $\Delta\delta$) and the desired brake force ($\frac{T_{bi}}{R}$), provided by the low level wheel slip controller. The input to the control algorithm are specified through the measurement block, where the vehicle

Numerical parameters	
ε	10^{-8}
Allocation tuning parameters	
W_π	$diag(1,1,1,1,5)$
W_u	$diag(2,2,2,2,3)10^3$
w_λ	0.1
w_δ	0.1
High and low level control parameters	
K_P	$15J_z$
K_I	$50J_z$
Γ_P	500
Actuator constraints	
$\lambda_{x\min}$	-10^{-4}
$\lambda_{x\max}$ (λ_{Dri})	$0.10+10^{-4}$
$\Delta\delta_{\max}$	$3[\deg]$
Adaptive algorithm	
$\gamma_{\mu i}$	1
$\gamma_{\bar{\lambda} i}$	0.2
A	30
λ_{Axi}	0.006

TABLE III
ALGORITHM PARAMETERS

states and variables are corrupted and delayed according to realistic vehicle sensor characteristics. In the figures and plots presented, only the actual states are given.

The results from the simulations of the three above mentioned scenarios are show in the Figures 10, 11 and 12. Furthermore, for the cases where only braking actuators and only steering actuator are considered, the fishhook maneuver simulation results are shown in Figures 13 and 14. The implementation of the braking only and steering only algorithms may be carried out by; (i) shrinking the actuator constraints of the actuators not considered, or (ii) by implementing two separate algorithms. The first approach offers a strategy for dynamic handling actuator failure or actuator efficiency reduction, since the constraints of the actuators may be continuously updated in the algorithm. However, care must be taken since the efficiency of the algorithm may be reduced, due to the fact that changing the constrains of one actuator may indirectly effect the update laws for the other actuators through the calculations of the Lagrangian parameter. This means that tuning the algorithm with time-varying gains $W_\pi(t)$ and $W_u(t)$ may be necessary. By the first strategy the simulation results shown in Figure 13 are generated by setting $\Delta\delta_{\max} = 3\cdot 10^{-4}[\deg]$ and $W_u = diag(2,2,2,2,3\cdot 10^2)10^3$, and the results in Figure 14 are generated by setting $\lambda_{x\max} = 10^{-4}$ and $W_u = diag(4,4,4,4,1)10^3$. Similar results may also in this special case be obtained by considering two separate algorithm implementations.

The main idea of the dynamic control allocation algorithm presented here is to provide a control allocation solution that; (i) converges to an optimal actuator constellation based on a static optimization problem formulation and, (ii) does not depend on any optimizing software. For the yaw rate control problem $r \to r_{ref}$, this imply the moment convergence chain: $\Phi_M(\delta+\Delta,\lambda_x,\alpha,\mu_H) \to \Phi_M(\delta+\Delta\delta,\lambda_x,\alpha,\hat{\mu}_H) \to \Phi_M(\delta+\Delta\delta,\lambda_{xd},\alpha,\hat{\mu}_H) \to M_c$, where the first part is related to the stability of the tire-road maximal friction estimate, the second part is related to the stability and convergence of the low level controller and the last part is related to the dynamic control allocation algorithm and its stability properties. As can be seen in the simulation examples, the parameter estimates converge when the persistence of excitation property is satisfied, further the longitudinal slips on each wheel converges to their references. And in the plots showing the yaw torque, the estimated (calculated by the control allocation algorithm) converges to the desired yaw torque M_c from the high level controller. The dotted lines in the torque plots are measurements of the real yaw torque. The reason for this torque not to converge to the estimated torque is due to modeling errors. These errors are related to both the model structure (ignoring restoring moments and damping) errors and uncertain environmental and vehicle parameters e.g. the surface, tire, and weight distribution parameters. In fact in the presented scenarios the vehicle body is a unknown black box model.

From the plots it can be seen that the control objectives are satisfied, over- and under steering prevented and steerability conserved. It should be noted that when the steering angle is used actively, less control forces are commanded to the wheel brakes, which means that the controlled maneuver will have less impact on the absolute velocity (see the first plots in the Figures 12 a), 13 a) and 14 a)), but at the same time it will slow down the estimation of the maximal tire-road friction parameters (last plots in the Figures 12 a), 13 a) and 14 a)). Furthermore, the maximal tire-road friction parameters are adapted only when the measured longitudinal wheel slips are high enough. Moreover the independence of the parameter estimates is shown in plot a.4 from the fishhook scenario (Figure 12), where the parameters associated to the right side of the vehicle are estimated related to a surface with high friction and the ones on the left side are related to a low friction surface. Also specifically note the transients at ca. $1.6s$ and $4.2s$ in yaw rate and the longitudinal wheel slip plots from Figure 12 a) and b). The first transient is due to surface changes (see the scenario description), and the second occur because the yaw stabilizing algorithm is switched off when no steering action is performed.

Finally note that more actuators suggest better performance, especially when actuators saturate, see Figures 12, 13 and 14 for a comparison and note the degenerated solution in the yaw torque plot where the steering actuator saturates.

VII. CONCLUSION

The focus of this work was on presenting the yaw stabilizing problem in the framework of a modular efficient dynamic control allocation scheme. The control allocation scheme does not rely on an exact optimization, but presents a dynamic optimization solution that converges to the optimum in a stable manner. This is suitable for over-actuated mechanical systems that require high reliability and low production cost, such as this automotive application. The modularity of the approach was shown by de-coupling the high level vehicle motion from the low level dynamics of the wheel slip with a control allocation scheme commanding desired longitudinal wheel slip and steering angle corrections. Furthermore the scheme was tested in a highly realistic proprietary simulation environment by DaimlerChrysler, and over- and under steering of the vehicle was efficiently prevented.

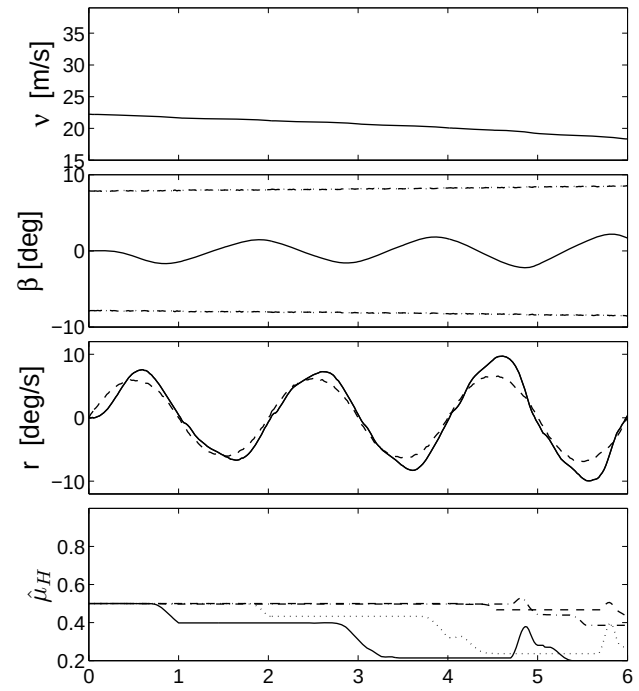

(a) System states. The dashed lines in plot 2 and 3 are given by $\beta_{\max}$ (8) and r_{ref} (7). In plot 4 the lines represent the following: solid-$\hat{\mu}_{H1}$, dotted-$\hat{\mu}_{H2}$, dashdot-$\hat{\mu}_{H3}$, dashed-$\hat{\mu}_{H4}$

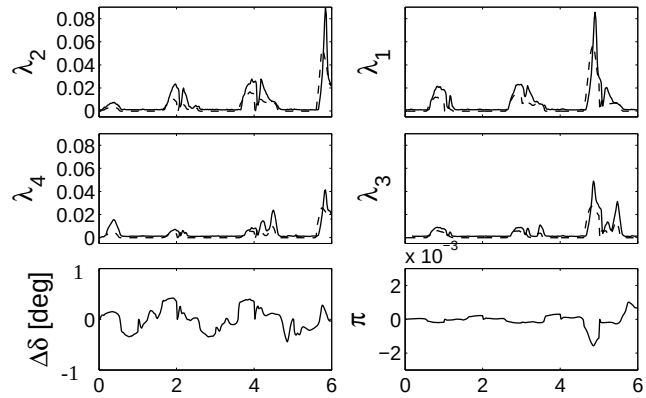

(b) The longitudinal wheel slip, the steering angle manipulation and lagrangian parameter. The dotted lines denote the desired longitudinal wheel slip.

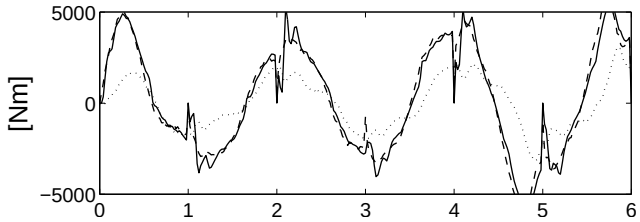

(c) Yaw torque: M_c-dashed, $M_{estimated}$-solid, M_{real}-dotted.

Fig. 10. The under steering scenario, with active yaw stabilization

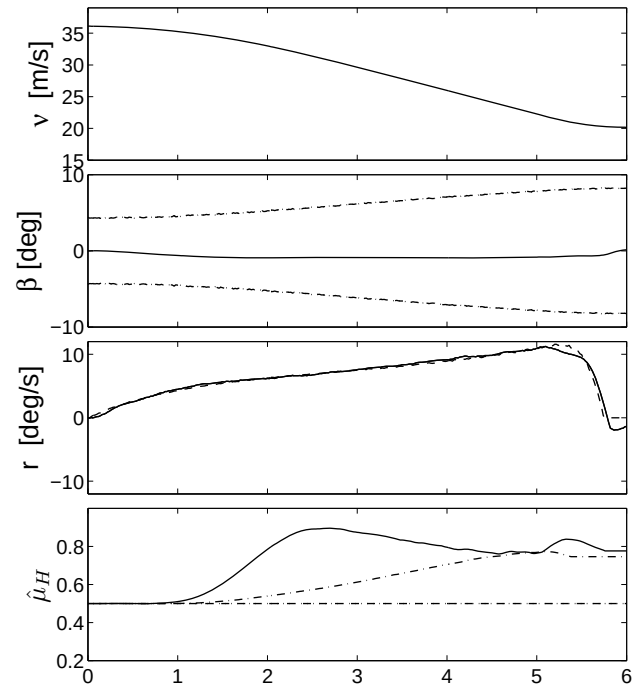

(a) System states. The dashed lines in plot 2 and 3 are given by $\beta_{\max}$ (8) and r_{ref} (7). In plot 4 the lines represent the following: solid-$\hat{\mu}_{H1}$, dotted-$\hat{\mu}_{H2}$, dashdot-$\hat{\mu}_{H3}$, dashed-$\hat{\mu}_{H4}$

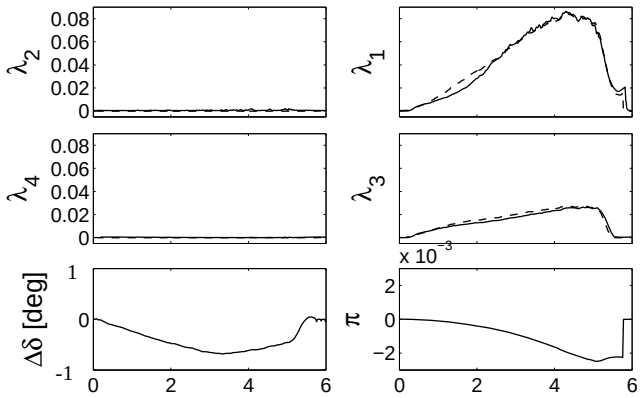

(b) The longitudinal wheel slip, the steering angle manipulation and lagrangian parameter. The dotted lines denote the desired longitudinal wheel slip.

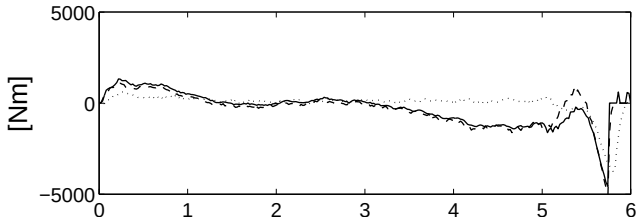

(c) Yaw torque: M_c-dashed, $M_{estimated}$-solid, M_{real}-dotted.

Fig. 11. The over steering scenario, with active yaw stabilization

Interesting further work involve a detailed performance analysis of the yaw stabilizing algorithm. Important topics in such analysis will be the evaluation and classification of the algorithm friction model. Further interesting topics are related to strategies with increased functionality (augmentation of rollover prevention) and robustness (by including additional actuators, for example through the pressure control of an active hydro pneumatic (AHP) suspension system). In the case of higher actuator redundancy, both improved performance and increased robustness of this yaw stabilizing system are expected. Also focus on algorithm validation with respect to analyzing noise and model error sensitivity should be consid-

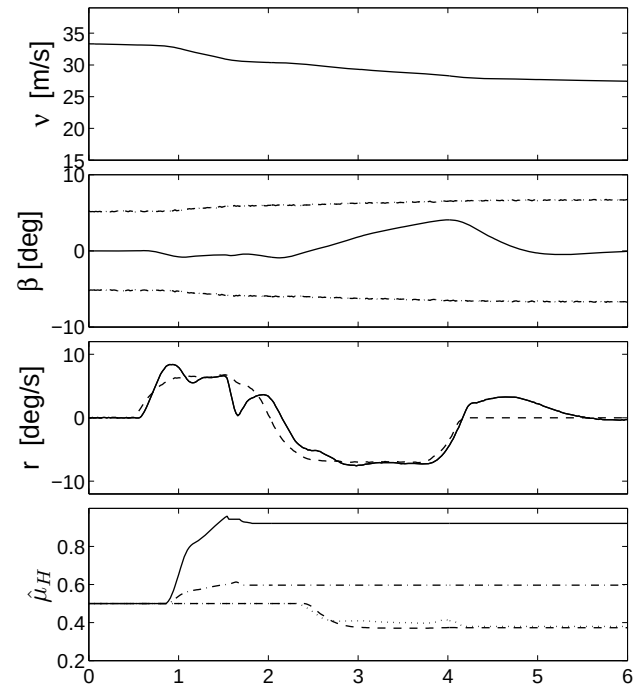

(a) System states. The dashed lines in plot 2 and 3 are given by $\beta_{\max}$ (8) and r_{ref} (7). In plot 4 the lines represent the following: solid-$\hat{\mu}_{H1}$, dotted-$\hat{\mu}_{H2}$, dashdot-$\hat{\mu}_{H3}$, dashed-$\hat{\mu}_{H4}$

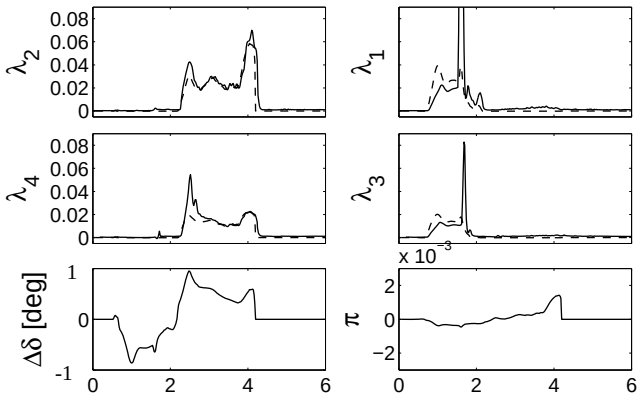

(b) The longitudinal wheel slip, the steering angle manipulation and lagrangian parameter. The dotted lines denote the desired longitudinal wheel slip.

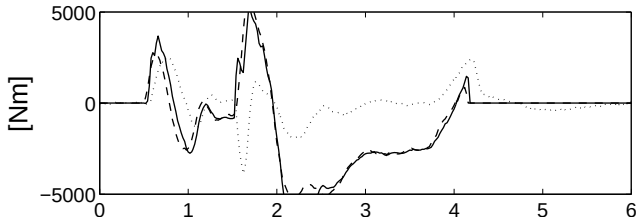

(c) Yaw torque: M_c-dashed, $M_{estimated}$-solid, M_{real}-dotted.

Fig. 12. The fishhook test, with active yaw stabilization

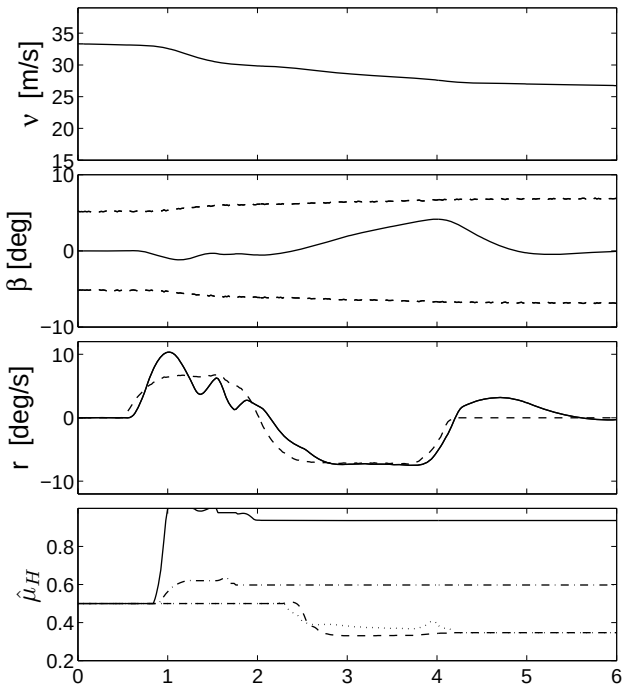

(a) System states. The dashed lines in plot 2 and 3 are given by $\beta_{\max}$ (8) and r_{ref} (7). In plot 4 the lines represent the following: solid-$\hat{\mu}_{H1}$, dotted-$\hat{\mu}_{H2}$, dashdot-$\hat{\mu}_{H3}$, dashed-$\hat{\mu}_{H4}$

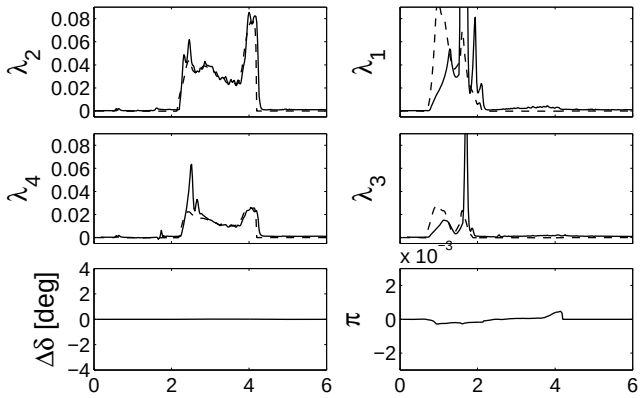

(b) The longitudinal wheel slip and lagrangian parameter (no the steering angle manipulation). The dotted lines denote the desired longitudinal wheel slip.

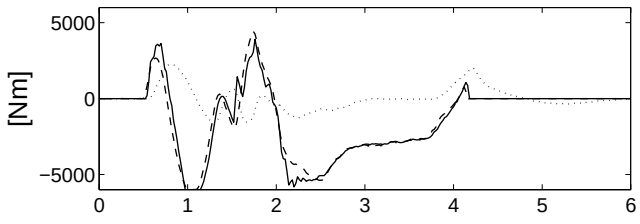

(c) Yaw torque: M_c-dashed, $M_{estimated}$-solid, M_{real}-dotted.

Fig. 13. The fishhook test, only active braking

ered. By including observer dynamic, additional transients are introduced in the scheme. These transients should be handled in the control algorithm for optimal performance. Although the robustness introduced by the UAS/UES properties of the algorithm handle uncertainties in the state estimates, the analysis and the specific performance requirements on state observers incorporated in the control allocation algorithm, are considered to be the main topics for further development of the proposed control allocation algorithm.

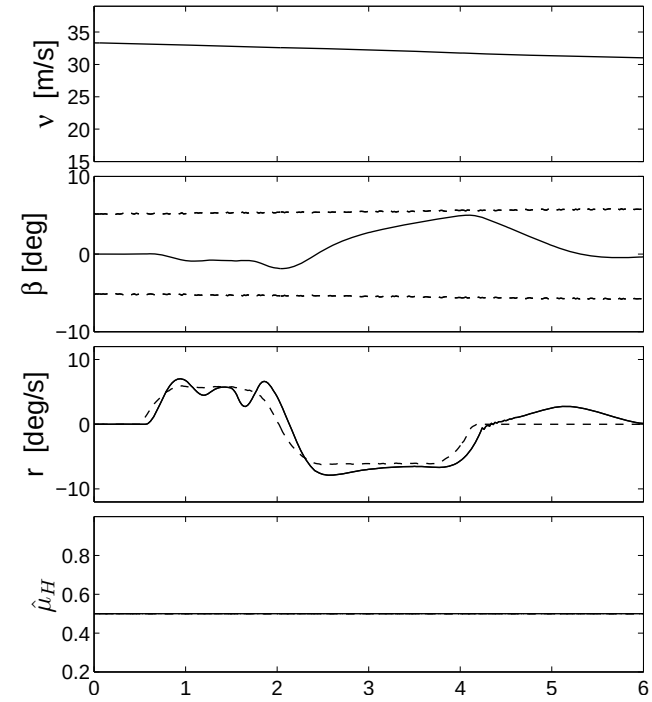

(a) System states. The dashed lines in plot 2 and 3 are given by $\beta_{\max}$ (8) and r_{ref} (7). In plot 4, there is no parameter estimation

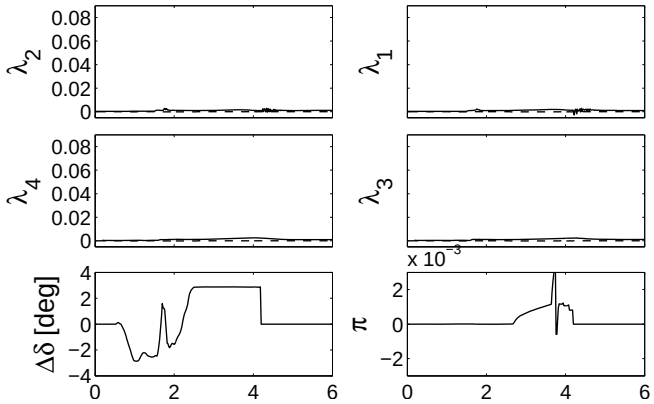

(b) The steering angle manipulation and lagrangian parameter. The dotted lines denote the desired longitudinal wheel slip.

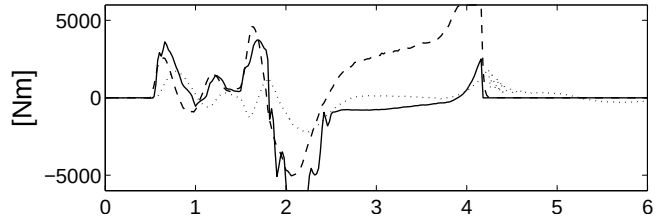

(c) Yaw torque: M_c-dashed, $M_{estimated}$-solid, M_{real}-dotted.

Fig. 14. The fishhook test, only active steering

VIII. Acknowledgments

The authors are grateful to Jens C. Kalkkuhl and Avshalom Sussia at DaimlerChrysler, and Lars Imsland and Petter Tøndel at SINTEF, for insightful comments. The work is sponsored by the Research Council of Norway through the Strategic University Program on Computational Methods in Non linear Motion Control and the European Commission through the STREP project CEmACS, contract 004175.

References

[1] J. Ackermann and T. Bünte. Handeling improvement of robust car steering. *in International Conference on Adcances in Vehicle Control and Safety*, 1998.

[2] J. Ackermann, J. Guldner, W. Sienel, R. Steinhauser, and V. Utkin. Linear and nonlinear controller design for robust automatic steering. *IEEE Transactions of Control Systems Technology*, 3(1):132–143, 1995.

[3] J. Ackermann, D. Odenthal, and T. Bünte. Adventages of active steering for vehicle. *in 32nd International Symposium on Automotice Technology and Automation*, pages 263–270, 1999.

[4] V. Alberti and E. Babbel. Improved driving stability of active braking of the individual wheels. *In Proc. of the International Symposium on Advanced Vehicle Control*, pages 717–732, 1996.

[5] F. Borrelli, P. Falcone, T. Keviczky, J. Asgari, and D. Hrovat. Mpc-based approach to active steering for autonomous vehicle systems. *International Journal on Vehicle Autonomous Systems*, 3:265–291, 2005.

[6] M. Burckhardt. *Fahrzeugmechanik: Radschlupf-Regelsysteme*. Vogel Fachbuch, Wüzburg, 1993.

[7] S. Choi and D.-W. Cho. Control of wheel slip ratio using sliding mode controller with pulse width modulation. *In Proc. 4th International Symposium on Advanced Vehicle Control, Nagoja, Japan*, pages 629–635, 1998.

[8] P. Falcone, F. Borrelli, J. Asgari, E. H. Tseng, and D. Hrovat. Predictive active steering control for autonomous vehicle systems. *IEEE Trans. Control Systems Technology*, 15:566–580, 2007.

[9] P. Falcone, F. Borrelli, J. Asgari, H. E. Tseng, and D. Hrovat. A model predictive control approach for combined braking and steering in autonomous vehicles. *15th Mediterranean Conference on Control and Automation, Athens, Greece*, 2007.

[10] R. Freeman. Robust slip control for a single wheel. Technical Report 2004-8-W, University of California, Santa Barbara, Santa Barbara, California, 1995.

[11] B. A. Guvenc, T. Acarman., and L. Guvenc. Coordination of steering and individual wheel braking actuated vehicle yaw stability control. *Proceedings of IEEE Intelligent Vehicles Symposium*, pages 288–293, 2003.

[12] Y. Hattori, K. Koibuchi, and T. Yokoyama. Force and moment control with nonlinear optimum distribution of vehicle dynamics. *in Proc. of the 6th International Symposium on Advanced Vehicle Control*, pages 595–600, 2002.

[13] L. Imsland, T. A. Johansen, T. I. Fossen, H. F. Grip, J. C. Kalkkuhl, and A. Suissa. Vehicle velocity estimation using nonlinear observers. *Automatica*, 42:2091–2103, 2006.

[14] L. Imsland, T. A. Johansen, T. I. Fossen, H. F. Grip, J. C. Kalkkuhl, and A. Suissa. Nonlinear observer for lateral velocity with friction and road bank adaptation validation and comparison with an extended kalman filter. *SAE World Congress, Detroit*, 2007.

[15] P. A. Ioannou and J. Sun. *Robust Adaptive Control*. Prentice Hall PTR, New Jersey, 1996.

[16] F. Jiang. *A novel approach to a class of antilock brake problems*. PhD thesis, Cleveland State University, 2000.

[17] T. A. Johansen. Optimizing nonlinear control allocation. *Proc. IEEE Conf. Decision and Control. Bahamas*, pages 3435–3440, 2004.

[18] T. A. Johansen, I. Petersen, J. Kalkkuhl, and J. Ludemann. Gain-scheduled wheel slip control in automotive brake systems. *IEEE Trans. Control Systems Technology*, 11:799–811, 2003.

[19] U. Kiencke and L. Nielsen. *Automotive Control Systems*. Springer-Verlag, 2000.

[20] S. Mammer and D. Koenig. Vehicle handeling improvement by active steering. *Vehicle System Dynamics*, 38(3):211–242, 2002.

[21] D. Piyabongkarn, R. Rajamani, J. Y. Lew, and Hai Yu. On the use of torque-biasing devices for vehicle stability control. *American Control Conference (ACC), Minneapolis, Minnesota, USA*, pages 5360–5365, 2006.

[22] J. H. Plumlee, D. M. Bevly, and A. S. Hodel. Control of a ground vehicle using quadratic programming based control allocation techniques. *in Proc. American Contr. Conf.*, pages 4704–4709, 2004.

[23] R. Rajamani. *Vehicle Dynamics and Control*. Springer New York, Veritasveien 1, N-1322, Høvik, Norway, 2006.

[24] R. Rajamani, D. Piyabongkarn, J. Y. Lew, and J. A. Grogg. Algorithms for real-titme estimation of individual wheel tire-road friction coefficients. *American Control Conference (ACC), Minneapolis, Minnesota, USA*, pages 4682–4687, 2006.

[25] J. Reimpell and P. Sponagel. *Fahrzeugmechanik: Reifen und Räder*. Vogel Fachbuch, Wüzburg, 1995.

[26] S. M. Savaresi and M. Tanelli. Mixed slip-deceleration control in automotive braking systems. *Journal of Dynamic Systems, Measurement, and Control*, 129:20–31, 2007.

[27] M. Schinkel and K. Hunt. Anti-lock braking control using a sliding mode like approach. *In Proc. American Contr. Conf., Anchorage*, 3:2386–2391, 2002.

[28] T. Shim and D. Margolis. Using μ feedforward for vehicle stability enhancement. *Vehicle System Dynamics*, 35(2):113–119, 2001.

[29] S. Solyom and A. Rantzer. *Nonlinear and Hybrid Control in Automotive Applications. Chapter ABS Control - A Design Model and Control Structure*. Springer-Verlag, New Jersey, 2002.

[30] S. Taheri and E. Law. Slip control braking of an automobile during combined braking and steering manoeuvres. *ASME Advanced Automotive Technologies*, 40:209–227, 1991.

[31] J. Tjønnås. *Nonlinear adaptive control allocation.* Phd thesis, NTNU, Trondheim, Norway, 2008.

[32] J. Tjønnås and T. A. Johansen. Adaptive optimizing dynamic control allocation algorithm for yaw stabilization of an automotive vehicle using brakes. *14th Mediterranean Conference on Control and Automation, Ancona, Italy*, 2006.

[33] J. Tjønnås and T. A. Johansen. On optimizing nonlinear adaptive control allocation with actuator dynamics. *7th IFAC Symposium on Nonlinear Control Systems, Pretoria, South Africa*, 2007.

[34] J. Tjønnås and T. A. Johansen. Adaptive control allocation. *Accepted in Automatica,* 2008.

[35] P. Tøndel and T. A. Johansen. Control allocation for yaw stabilization in automotive vehicles using multiparametric nonlinear programming. *American Control Conference, Portland*, 2005.

[36] A. T. van Zanten, R. Erhart, and G. Pfaff. The vehicle dynamics control system of BOSCH. *SAE 950759*, 1995.

[37] J. Wang and D. A. Crolla D. A. Wilson, W. Xu. Active suspension control to improve vehicle ride and steady-state handling. *Proceedings of the 44th IEEE Conference on Decision and Control, and the European Control Conference*, pages 1982–1987, 2005.

[38] J. Wang and R. G. Longoria. Coordinated vehicle dynamics control with control distribution. *American Control Conference (ACC), Minneapolis, Minnesota, USA*, pages 5348–5353, 2006.

[39] M. C. Wu and M. C. Shih. Hydraulic anti-lock braking control using the hybrid sliding-mode pulse width modulation pressure control method. *Proc. Instn. Mech. Engrs. 215*, pages 177–187, 2001.

[40] J. S. Yu. A robust adaptive wheel-slip controller for antilock brake system. *In Proc. 36th IEEE Conf. on Decision and Control, San Diego, USA*, pages 2545–2546, 1997.

[41] S. H. Yu and J. J. Moskwa. A global approach to vehicle control: Coordination of four wheel steering and wheel torques. *Journal of dynamic systems, measurement, and control*, 116:659–667, 1994.